

STUDY ON THE EFFECT OF AERATED LUBRICANT ON THE JOURNAL TRACES IN THE ENGINE BEARING CLEARANCE

S. JANG^{1)*} and Y. PARK²⁾

¹⁾School of Mechanical and Automotive Engineering, Kookmin University, Seoul 136-171, Korea

²⁾Graduate School of Automotive Engineering, Kookmin University, Seoul 136-171, Korea
(currently at Biomechatronic Lab. Institute of Industrial Technology, Korea University, Seoul 136-701, Korea)

(Received 8 July 2004; Revised 3 November 2004)

ABSTRACT—This work analyzes the behaviors of aerated lubricant in the gap between con-rod bearing and journal. It is assumed that the film formation with aerated lubricant is influenced by the two major factors. One is the density characteristics of the lubricant due to the volume change of lubricant for the formation of bubbles and the other is the viscosity characteristics of the lubricant due to the surface tension of the bubble in the lubricant. These two major factors surprisingly increase the load capacity in some ranges of bubble sizes and densities. Modified Reynolds' equation is developed for the computation of fluid film pressure with the effects of aeration ratio in the lubricant. From the calculated load capacity by solving modified Reynolds' equation, journal locus is computed with Mobility method after comparing it with the applied load at each time step. The differences of journal orbits between aerated and pure lubricants are shown in the computed results.

KEY WORDS : Aeration, Big-end bearing, Mobility method, Journal traces, Load capacity

1. INTRODUCTION

The aeration in the lubrication system of engine frequently happens with many kinds of bubble sizes. Whenever the lubricant sprays due to the rotational movement of the components and oil starvation is made in the small gap due to the relative motions of the components, air is dissolved under the condition of atmosphere pressure and makes bubbles inside of the lubricant. In addition, the structure of oil circuits such as oil gallery and oil pump in the engine accelerates the aeration of the lubricant. At this moment, the aeration makes the shapes of bubbles sizing 1–100 μm scale. Both the number and the size of bubble greatly change the characteristics of lubricant, especially viscosity and density (Chamnprasart, 1993), which are the most important mechanical characteristics of lubricant.

Many researches have shown that the aeration is considered undesirable for the lubricating mechanism, because the bubbles collapse the fluid film and then the load capacity of fluid film is not made. However, recent research (Nicolajsen, 1999a and b) analytically verifies that the surface tension force of the bubble in the lubricant increases the apparent viscosity although it decreases the density of the lubricant. Therefore, the load

capacity of the aerated lubricant is verified to be larger than that of pure lubricant by solving the developed Reynold's equation due to the enlarged apparent viscosity. In Nicolajsen's research (1999a and b), the load capacity is computed with the assumptions of the short bearing theory and the steady state condition, which are just simple ideal cases of journal bearing system.

The engine bearing is operated under the condition of highly fluctuating loads and is imposed by very large fluid film pressure around the bearing during the engine cycle. These operating conditions differentiate the aeration behaviors from those of steady state condition and analysis of dynamic loading system will give more realistic information for the clearance behaviors of the aerated lubricant.

In this work, the journal locus of engine bearing is analyzed under the dynamic loading condition because the engine bearing is one of the most severely loaded components in the engine. In our analysis, the pressure gradients of both the radial and width directions are simultaneously considered by solving the modified Reynolds' equation for the aerated lubricant behaviors. The ratio of width and diameter of bearing, bubble size and aeration ratio are the major input values in the computation of fluid film pressure distribution over the bearing area. The dynamic equation for the computation of journal locus in the bearing clearance is obtained by

*Corresponding author. e-mail: jangs@kookmin.ac.kr

the Mobility method after the fluid film pressure over the bearing area is computed with the modified Reynolds' equation.

2. MODEL OF THE AERATED LUBRICANT

The apparent viscosity and density of the aerated lubricant are modeled with the following assumptions.

- (1) The aerated air in the lubricant is considered as the ideal gas.
- (2) The bubbles are evenly distributed and don't touch each other.

The shape of the aerating bubbles in the lubricant is shown in Figure 1. The aerated ratio is described as the term r/d and the whole amount of air in the lubricant is $(400p/3) (r/d)^3$ [%]. The most significant characteristics of the bubble is that it sustains its spherical shape due to the surface tension. Therefore, it causes the increase of shear resistance when the bubble surfaces are sheared and

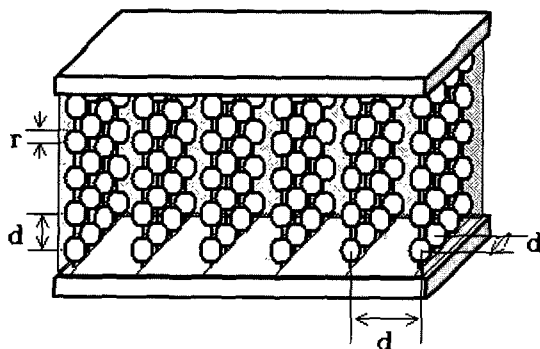


Figure 1. Schematic diagram of aerated lubricant film modeling.

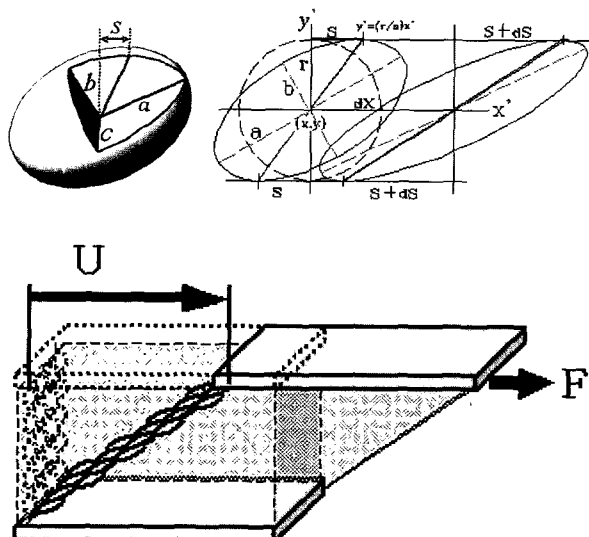


Figure 2. Bubble distortion shape due to shear flow.

finally the apparent viscosity increases. The apparent viscosity of bubbled fluid is very delicately influenced by the physical dimensions of the bubbles, which in turn influence the clearance behaviors of moving components in the engine.

With the assumptions of no slip boundary condition at the interface between solid surface and fluid as well as the variation of surface area, the bubble distortion is simulated by Figure 2.

The surface of the distorted bubble is computed by the surface integral form.

$$A = 8 \int_0^{\frac{\pi}{2}} \int_0^{\frac{\pi}{2}} (\alpha^2 b^2 \cos^4 \theta \cos^2 \phi v + a^2 c^2 \cos^4 \theta \sin^2 \phi + b^2 c^2 \sin^2 \theta \cos^2 \theta)^{1/2} d\theta d\phi \quad (1)$$

The major and minor axes are calculated with initial sphere diameter of bubble r .

$$a = \sqrt{\frac{1}{2}(2r^2 + s^2 + s\sqrt{s^2 + 4r^2})} \quad (2)$$

$$b = \sqrt{\frac{1}{2}(2r^2 + s^2 - s\sqrt{s^2 + 4r^2})} \quad (3)$$

Substituting equation (2) and (3) into (1) gives the rate of surface area increase by Simpson's rule of numerical integration. The integrated result is shown in the Figure 3 and the increase rate with the ratio of s/r is computed to be 6.1157.

The work of surface area distorting ΔW_x is defined by the surface tension s and area increase ΔA as following.

$$\sigma = \frac{\Delta W_x}{\Delta A} \quad (4)$$

The surface distorting work is defined by the multiplication of distortion force and distorted displacement of

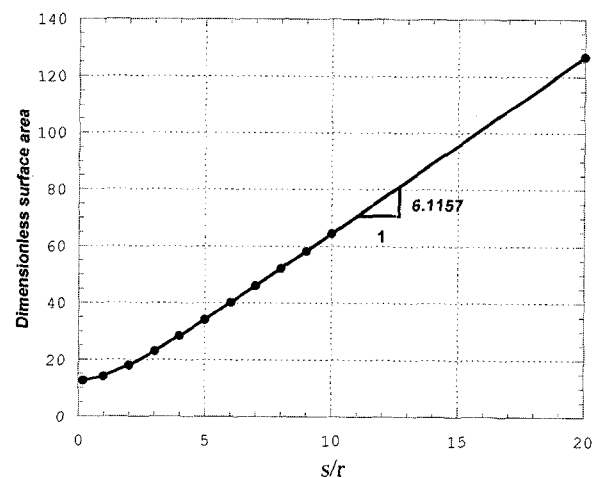


Figure 3. Surface area increase rate by the distortion ratio s/r .

bubble (Streeter, 1958).

$$\Delta W_x = \Delta F_x \Delta X_h = \Delta F_h (U \Delta t) \quad (5)$$

Substituting equation (5) into (4) gives the relationship between shear resistance force ΔF_x and shear rate $\Delta s / \Delta t$ of bubble distorted displacement as equation (6).

$$\Delta F_x = \frac{\sigma \Delta A}{U \Delta t} = 6.1157 r \left(\frac{\sigma}{U} \right) \frac{\Delta s}{\Delta t} \quad (6)$$

The shear rate $\Delta s / \Delta t$ of bubble distorted displacement is computed by the combination of Couette and Poiseuille flows as below equation (7).

$$u(y) = \frac{1}{2\mu} \frac{dp}{dx} (y^2 - yh) + \frac{Uy}{h} \quad (7)$$

The mean shear rate at the location of at $y+r$ and $y-r$ is the ratio of velocity difference to give time Δt as equation (8).

$$\frac{\Delta s}{\Delta t} = \frac{u_{y+r} - u_{y-r}}{2} = \left[\frac{u_h}{h} + \frac{2y-h}{2\mu} \frac{\partial P}{\partial x} \right] r \quad (8)$$

Therefore, the shear resistance force is expressed by the following form by using equations (6), (7) and (8). (Nicolajsen, 1999a and b)

$$\Delta F_x = 6.1157 r^2 \sigma \left[\frac{1}{h} + \frac{2y-h}{2\mu U} \frac{\partial P}{\partial x} \right] \quad (9)$$

, where r is the radius of bubble, σ and μ are surface tension and viscosity of the lubricant, respectively and U is the relative velocity of solid surface.

As the aeration ratio increases, the density of aerated lubricant decreases because of the volume of bubble in the lubricant. The proposed density model is related to the surface tension and the viscosity of lubricant. The dimensionless internal pressure of the bubble in the pressurized region is described by the following equation (10) with the surface tension property and the internal gas pressure of the bubble is related to the ideal gas equation:

$$P_{air}^* = p_{oil}^* + 2 \frac{\sigma}{r} \quad (10)$$

The mass ratio between air and oil in the lubricant is expressed as equation (11) and substitution of it into equation (10) gives the density model of the aerated lubricant. Therefore, the density of the aerated lubricant is expressed as the following dimensionless form, equation (14):

$$\eta = \frac{m_{air}}{m_{oil}} = \frac{\rho_{air} V_{air}}{\rho_{oil} V_{air}} = \frac{(\rho_{air})_{in} \frac{4}{3} \pi r^3 N}{\rho_{oil} \left(V_{in} \frac{4}{3} \pi r^3 N \right)} = \frac{P_{air}^*}{\left\{ \left(\frac{3}{4\pi} \right) \left(\frac{d_{in}}{r_{in}} \right) - 1 \right\}} \quad (11)$$

$$p_{oil} = \rho_{oil} \tilde{R} T \quad (12)$$

$$p_{air}^* = \frac{p_{air}}{p_{oil}} = \frac{p_{air}}{\rho_{oil} \tilde{R} T} \quad (13)$$

$$\rho^* = \frac{\rho_{air}}{\rho_{oil}} = \frac{m_{oil} + m_{air}}{\rho_{oil} (V_{oil} + V_{air})} = \frac{1 + \eta}{1 + \eta (\rho_{oil} \tilde{R} T / p_{air}^*)} \quad (14)$$

$$= \frac{p_{air}^* (1 + \eta)}{p_{air}^* + \eta}$$

As the viscosity of the incompressible lubricant without aeration strongly depends on the variation of temperature, the viscosity of the aerated lubricant varies for many other operational conditions. In this work, the viscosity model of the aerated lubricant considers only two effects. The one is the term caused by the aeration volume, which influences the density of the whole lubricant. The apparent viscosity by the density change is expressed by the following:

$$\mu_1^* = \frac{\rho^*}{1 + \eta} \quad (15)$$

The other is the shear behavior of pressurized fluid film that causes the deformation of each bubble inside of the lubricant, which eventually changes the surface tension of the bubble.

The shear resistance by shearing behaviors increases the apparent viscosity and is described by the following equation (16).

$$\mu_2^* = 6.1157 \left(\frac{\sigma r^{*2} \xi}{\mu_{oil} U r_{in}^{*3}} \right) \left(\frac{r_{in}^*}{d_{in}^*} \right)^3 \sqrt{\frac{h_{in}^{*3}}{h^*}} \quad (16)$$

where,

$$\xi = 1 + \frac{h(2y-1)}{2\mu_{oil} U} \frac{\partial P}{\partial x} \quad (17)$$

The apparent viscosity is the summation of the variation

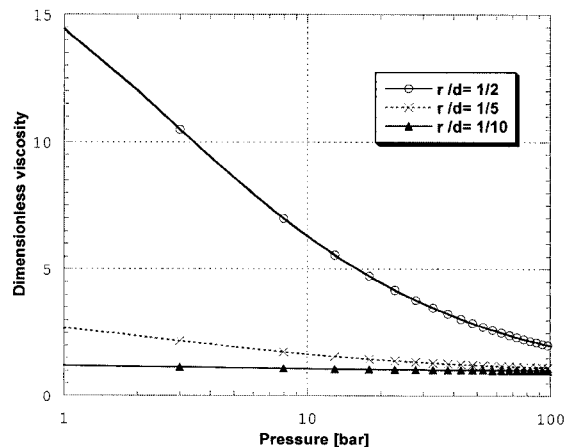


Figure 4. Apparent viscosity changes of aerated lubricant according to the variation of applied pressure.

of viscosity due to the density change as well as the surface tension by the shear behavior. The final form of the viscosity modeling for the aerated lubricant is expressed by the following equation:

$$\mu^* = \mu_1^* + \mu_2^* = \left[\frac{\rho}{1 + \eta} \right] + \left[6.1157 \left(\frac{\sigma r^{*2} \xi}{\mu_{oil} u_h r_{in}^{*3}} \right) \left(\frac{r_{in}^*}{d_{in}^*} \right)^3 \sqrt{\frac{h_{in}^{*3}}{h^*}} \right] \quad (18)$$

The apparent viscosity described by the above equation (18) according to the applied pressure is shown in the Figure 4.

3. COMPUTATION OF BOTH FLUID FILM PRESSURE AND JOURNAL ORBIT

The journal locus in the bearing clearance is computed by solving the force equilibrium between applied force and load capacity of fluid film pressure, after the integration of the pressure distribution over the bearing area is performed. In Figure 5, the clearance formation between bearing and journal is shown and the fluid film pressure over the bearing area in that clearance is obtained by solving the following modified Reynolds' equation (19),

$$\begin{aligned} & \frac{\partial}{\partial \theta} \left(\Gamma \frac{\partial \Pi}{\partial \theta} \right) + \left(\frac{R}{L} \right)^2 \frac{\partial}{\partial z^*} \left(\Gamma \frac{\partial \Pi}{\partial z^*} \right) - \frac{3 \Pi}{2 h^{*3/2}} \left\{ \frac{\partial}{\partial \theta} \left(\Gamma h^{*1/2} \frac{\partial h^*}{\partial \theta} \right) \right\} \\ & = \left(\frac{6 \Lambda (\omega_a + \omega_b)}{h^{*3/2}} \right) \frac{\partial}{\partial \theta} (\rho^* h^*) + \left(\frac{12 \Lambda \omega_a}{h^{*1/2}} \right) \frac{\partial \rho^*}{\partial t^*} \quad (19) \\ & + \left(\frac{12 \Lambda \rho^* \omega_a}{h^{*3/2}} \right) \left[\frac{d\varepsilon}{dt^*} \cos \theta + \varepsilon \frac{d(\phi + \psi)}{dt^*} \sin \theta \right] \end{aligned}$$

where, the dimensionless values are the followings. (Hamrock, 1994)

$$\begin{aligned} z^* &= z/L, \quad h^* = h/c, \quad \Gamma = \frac{\rho^*}{\mu^*}, \quad t^* = \omega_a t, \\ p^* &= p/(F/LD), \quad \mu^* = \frac{\mu}{\mu_{oil}}, \quad \rho^* = \frac{\rho}{\rho_{oil}}, \quad (20) \\ \Pi &= p^* h^{*3/2}, \quad \Lambda = \frac{\mu_{oil} LD}{F} \left(\frac{R}{c} \right)^2 \end{aligned}$$

For the steep change of pressures near the minimum film thickness region where the computational stability is always issued, the dimensionless pressure is transformed into Π ($\Pi = p^* h^{*3/2}$) term, which attenuates the steep variation of fluid film pressure by relating the high fluid film pressure to the thin film thickness.

Using the computed pressure distribution of the fluid film, the load capacity is obtained by integrating the pressure distribution over the bearing area. The inverse

term of load capacity is regarded as the Mobility value. In this work, we make the Mobility values at every time step during the engine cycle and they include the effects of the behaviors of aerating bubbles for any ratio of B/D . The load capacity calculated from the pressure distribution of lubricant film is compared with the applied load at every time step of the cycle. Solving the equations of forces balance gives the information of the journal position in the clearance at a certain time step as well as squeezing and rotational velocities ($d\varepsilon/dt^*$, $d\phi/dt^*$) of journal center for the next time step. It is a kind of marching-out problem (Booker, 1965), which can be easily solved by fourth Runge-Kutta method. The balance between applied load and load capacity in ε and ϕ directions are described by the following equations (21) and (22).

$$F_\varepsilon = F \cos \phi = - \int_s P \cos \theta \, ds = -W_\varepsilon \quad (21)$$

$$F_\phi = F \sin \phi = - \int_s P \sin \theta \, ds = -W_\phi \quad (22)$$

The Mobility values in Equations (23) and (24) are defined and the directional values are shown in Figure 6.

$$M = \frac{2}{W} = \frac{2}{\sqrt{W_\varepsilon^2 + W_\phi^2}} \quad (23)$$

$$M_\varepsilon = M \cos \alpha, \quad M_\phi = -M \sin \alpha \quad (24)$$

$$\dot{\varepsilon} = \left(\frac{M_\varepsilon}{\Lambda} \right), \quad \dot{\phi} + \dot{\psi} - \left(\frac{\omega_a + \omega_b}{2} \right) = \left(\frac{M_\phi}{\Lambda} \right) \quad (25)$$

With these above values, the modified Reynold's

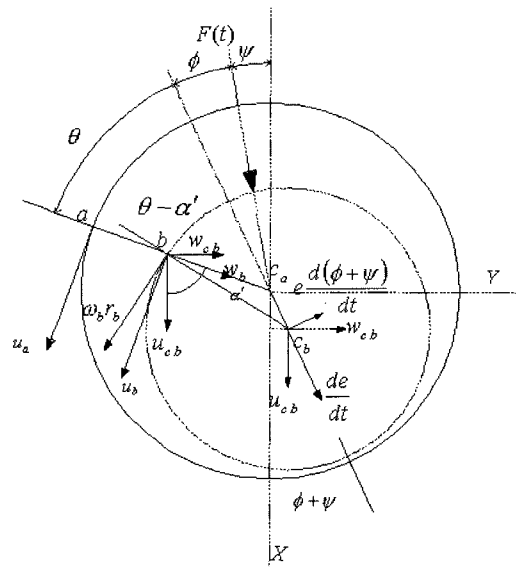


Figure 5. Film Geometry and velocity components in the dynamically loaded journal bearing.

Table 1. Input values for the computation of fluid film pressure of aerated lubricant.

Input parameter	Values
Engine speed	3000 rpm
Oil inlet pressure	1.0 bar
Journal diameter	0.045m
Viscosity (non-aerate oil)	0.0411 Pas
Density (non-aerate oil)	870.0 Kg/m ³
Surface tension of oil	0.0365 N/m
Clearance	80.0 μm
Oil temperature	353.15 K

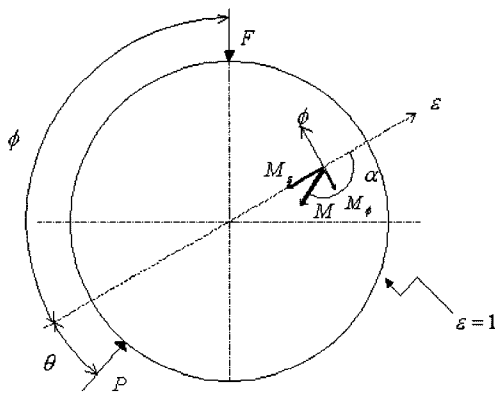


Figure 6. Representation of Mobility vector and its components.

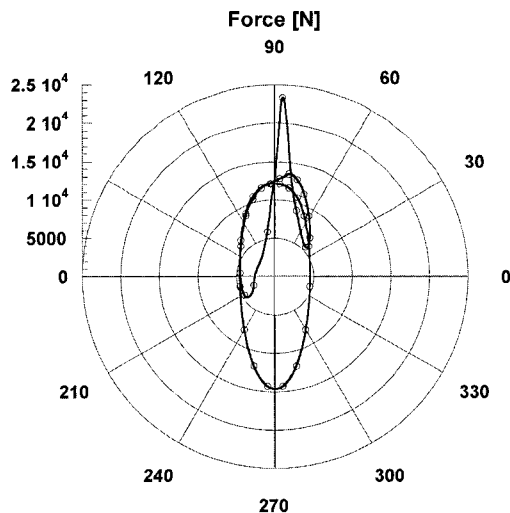


Figure 7. Applied loads variations on the big-end bearing at 3000 rpm of engine speed.

equation (19) is expressed in the following equation (26). This is the final form of the modified Reynold’s equation which describes the aerated lubricant behavior in the bearing clearance under the dynamic loading condition.

$$\frac{\partial}{\partial \theta} \left(\Gamma \frac{\partial \Pi}{\partial \theta} \right) + \left(\frac{R}{L} \right)^2 \frac{\partial}{\partial z^*} \left(\Gamma \frac{\partial \Pi}{\partial z^*} \right) - \frac{3 \Pi}{2 h^{*3/2}} \left\{ \frac{\partial}{\partial \theta} \left(\Gamma h^{*1/2} \frac{\partial h^*}{\partial \theta} \right) \right\} = \left(\frac{6 \Lambda (\omega_a + \omega_b)}{h^{*1/2}} \right) \left(\frac{\partial \rho^*}{\partial \theta} \right) + \left(\frac{12 \Lambda \omega_a}{h^{*1/2}} \right) \left(\frac{\partial \rho^*}{\partial t^*} \right) + \left(\frac{12 \rho^* \omega_a}{h^{*3/2}} \right) M \cos(\theta + \alpha) \quad (26)$$

4. RESULTS

The input values for the computation of journal locus in the bearing clearance are shown in Table 1. The applied load, Figure 7 during the cycle (3000 rpm) is depicted in polar coordinates. In case of pure lubricant, the conventional Reynold’s equation for the lubricant of constant density and viscosity is solved and the load capacity is converted into Mobility value at each time step. This is more general computational way to get the traces of journal center in the bearing clearance without using the Mobility map (Mobility database) which is not flexible both for various B/D ratios and the analysis of journal locus with non-linear characteristics of lubricant. In this work, the traces of journal center in the clearance are calculated according to the various width to diameter ratio (B/D) of the bearing. As the ratio of B/D increases in Figure 8, the load capacity has larger values and therefore, the eccentricity of journal center trace becomes

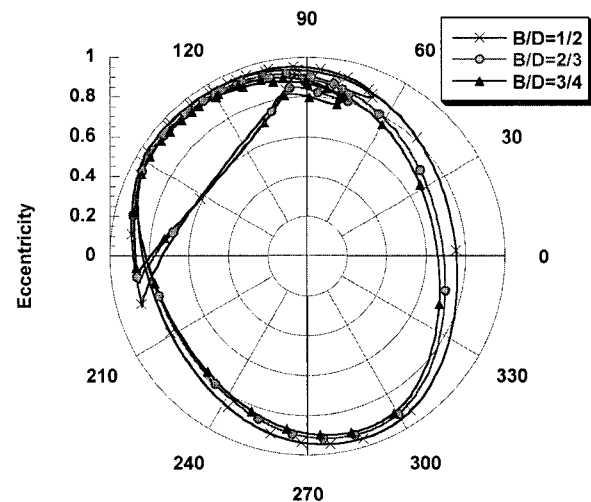


Figure 8. Journal center traces in the bearing clearance for non-aerated lubricant according to various B/D ratios at 3000 rpm of engine speed.

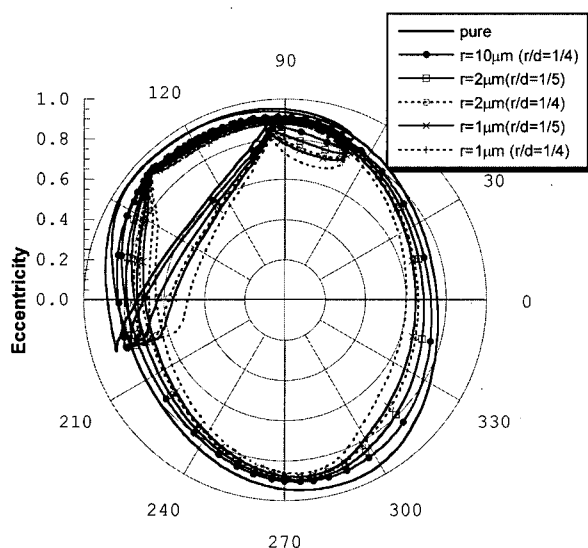


Figure 9. Journal center traces in the bearing clearance for aerated lubricant according to various bubble size to bubble distance ratios at $B/D=0.5$ at 3000 rpm of engine speed.

smaller during the cycle.

In case of aerated lubricant, smaller bubble size has higher load capacity under the same amount of air in the lubricant. This is the reason that smaller bubble size makes larger surface area of bubbles, which causes higher surface tension force. Larger surface tension increases apparent viscosity and therefore, the load capacity increases as the bubble size becomes smaller under the same amount of air in the lubricant. In Figure 9,

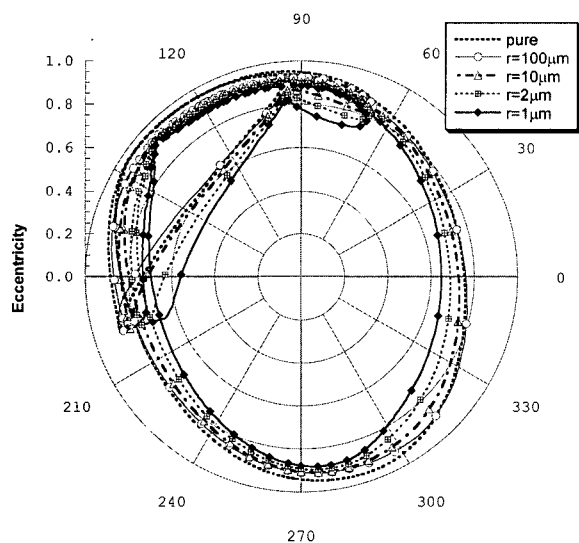


Figure 10. Journal center traces in the bearing clearance for aerated lubricant according to various bubble size at $B/D=0.5$ and $r/d=0.2$ at 3000 rpm of engine speed.

journal traces for the case of aerated lubricants are compared with those of the case of pure lubricant. In most cases, surface tension of bubbles in the lubricant makes the load capacity larger and the eccentricity of aerated lubricant shows smaller eccentricity than those of pure lubricant, while most researches have expected that bubbles in the lubricant makes the fluid film collapsed into no load capacities of lubricant film over the bearing area regardless of its sizes.

The load capacities of bearing according to the bubble sizes from 1 to 100 μm are computed and the results are shown in the Figure 10. Under the condition of the same amount of air in the lubricant, the small bubble sized lubricant has larger total surface area of bubbles than large size bubbled lubricant. This means that small size bubbled lubricant has more surface tension than large sized bubbled lubricant. Therefore, the apparent viscosity of small size bubbled lubricant is larger than that of large sized bubbled lubricant. This is the reason that load capacity of small size bubbled lubricant ($r = 1 \mu\text{m}$) is larger than those of the other cases and the journal trace of small size bubbled lubricant (1 μm) shows thicker film thickness than that of large size bubbled lubricant (100 μm) which depicts almost the same journal trace of non-aerated lubricant.

5. CONCLUSION

In this work, we developed the lubrication theory under the dynamic loading condition for the aerated lubricant of which the bubble size is about 1–100 μm and where the total amount of air is below 10% of the volume of lubricant. The pressure distributions over the bearing area are computed by solving the modified Reynolds' equation which considers the effect of bubble behaviors in the lubricant. For the journal locus, the applied load is compared with the load capacity in terms of Mobility value. From the computed results, we find that aerated lubricant has higher load capacity than pure lubricant under the dynamic loading condition. This is the reason that smaller bubble size makes more surface area, which eventually causes larger surface force and apparent viscosity. However, the above finding in this computation is based on the assumption that the bubble never collapses. Otherwise, it might cause the fluid flow resistance and the surface damages such as cavitation erosion, oxidation, fluid flow resistance.

ACKNOWLEDGEMENT—This work was supported by 2004 Kookmin University Research Fund.

REFERENCES

Booker, J. F. (1965). Dynamically loaded journal bearing:

- Mobility method of solution. *ASME J. Basic Engineering* **87**, **3**, 537–546.
- Chamnprasart, K., Al-Sharif, A., Rajagopal, K. R. and Szeri, A. Z. (1993). Lubrication with binary mixtures: bubbly oil. *J. Tribology*, **115**, 253–260.
- Hamrock, B. J. (1994). *Fundamentals of Fluid Film Lubrication*. McGraw-Hill. New York.
- Nikolajsen, J. L. (1999a). The effect of aerated oil on the load capacity of a plain journal bearings. *STLE, Tribology Transactions* **42**, **1**, 58–62.
- Nikolajsen, J. L. (1999b). Viscosity and density models for aerated oil in fluid-film bearings. *Tribology Trans.*, **42**, 186–191.
- Streeter, V. L. (1958). *Fluid Mechanics*. McGraw-Hill. New York.